X-ray study of strains and dislocation density in epitaxial Cu/Ni/Cu/Si(001) films

K. Ha, M. Ciria, and R. C. O'Handley
Department of Materials Science and Engineering, Massachusetts Institute of Technology, Cambridge, Massachusetts 02139

P. W. Stephens and S. Pagola
Department of Physics and Astronomy, State University of New York, Stony Brook, New York 11794-3800

(Received 16 April 1999; revised manuscript received 12 August 1999)

The strain state of epitaxial Cu(50 Å)/Ni(t_{Ni})/Cu(2000 Å)/Si(001) films as a function of the nickel film thickness (30 Å$\leqslant t_{Ni} \leqslant$2000 Å) has been studied using Bragg diffraction and grazing-incidence diffraction with a synchrotron x-ray source. For 30 Å$\leqslant t_{Ni} \leqslant$150 Å both the in-plane and out-of-plane nickel strains show a phenomenological $(1/t)^{2/3}$ power dependence, which is significantly different from the $1/t$ law commonly accepted in the literature. The Matthews' theory, including the effect of the copper capping layer, is used to account for the equilibrium strains of the nickel layer. The 500 and 2000 Å films show larger strains than that predicted by the theory, consistent with other studies. The ratio of the nickel in-plane to out-of-plane strains is -1.18 ± 0.05, very close to the expected nickel bulk value of $-2c_{12}/c_{11}=-1.28$. [S0163-1829(99)12743-7]

I. INTRODUCTION

The effect of strain on magnetism, namely inverse magnetostriction, can be significant in thin films and multilayers. Perhaps the most dramatic manifestation of this effect is the existence of strong perpendicular magnetization in the epitaxial Cu/Ni/Cu(001) system over a broad range of the nickel film thickness: the nickel magnetic moment prefers to point out of the plane of the film for the nickel film thickness ranging from 20 to 120 Å.[1–3] The broad range of the perpendicular magnetic anisotropy is due in part to the large residual strain in the nickel layer, which interacts with the magnetic moment through the magnetoelastic coupling. The resulting magnetoelastic anisotropy energy (which favors out-of-plane magnetization) can overcome the shape anisotropy (which favors in-plane magnetization). Because the strain-induced anisotropy is a product of the magnetoelastic coupling coefficient and strain, both quantities must be known if the magnetic anisotropy is to be understood and controlled. In this paper, the strain state of the nickel layer is described; the strength of the magnetoelastic coupling has been discussed elsewhere.[3]

Although there have been studies in the past on the strain of the nickel layer as a function of the nickel film thickness, they are inadequate for the study of the effect of inverse magnetostriction. For example, Chang[4] investigated the out-of-plane strain of the nickel in Cu(1000 Å)/Ni(t_{Ni})/Cu(1000 Å)/Si(001) films using x-ray diffraction. Since only a small number of samples ($t_{Ni}=50$, 100, 500, and 1000 angstroms) was investigated, little quantitative information about the strain behavior could be extracted from the data, particularly in the thickness range over which out-of-plane magnetization occurs. Another study by Müller *et al.*[5] used low-energy electron diffraction (LEED) to investigate the strain of ultrathin nickel films. Although LEED is useful for the study of surface reconstruction and relaxation, it is not suitable for investigating the average strain of films that are more than about ten-monolayers thick. In addition to having a broad range of perpendicular magnetic anisotropy, the Cu/Ni/Cu(001) system is a good candidate for the study of strain relaxation in metallic films. The materials are simple metals. The misfit strain of the nickel on copper is about 2.6%, not too large that it could prohibit epitaxial growth. In fact, the Ni/Cu(001) system was one of the first systems used to study the misfit accommodation in thin films.[6,7]

In this paper we present a strain study of Cu(50 Å)/Ni(t_{Ni})/Cu(2000 Å)/Si(001) films as a function of the nickel film thicknesses (30 Å$\leqslant t_{Ni} \leqslant$2000 Å) using synchrotron x-ray diffraction. The in-plane and out-of-plane strains were measured using the grazing-incidence diffraction (GID) and Bragg diffraction, respectively. For 30 Å $\leqslant t_{Ni} \leqslant$150 Å, both the in-plane and out-of-plane strains show a phenomenological $(1/t)^{2/3}$ power dependence, which is significantly different from the $1/t$ dependence commonly assumed in the literature.[8] The effect of the capping layer on the nickel is included by using the model proposed by Basson and Ball[9] (BB) (which is an extension of the Matthews' equilibrium strain model[10]). Large deviation from the equilibrium strain is observed in the 500 and 2000 Å films in agreement with other results.[6,7] The ratio of the in-plane to out-of-plane strain for the nickel films has the average value of -1.18 ± 0.05, which is in good agreement with the ratio $2c_{12}/c_{11}$ deduced for a film under biaxial stress induced by the epitaxial growth: the bulk elastic constants give $2c_{12}/c_{11}=1.28$.

II. SAMPLE PREPARATION

The silicon substrates were dipped in dilute hydrofluoric solution (5% by volume) for ten seconds to remove the native oxide. They were then rinsed in de-ionized water for about 3 min and immediately transferred into a load-lock chamber to be pumped down. The films were grown in a molecular-beam epitaxy chamber by *e*-beam evaporation. The base pressure was less than 2.0×10^{-10} torr. The deposition pressures for the copper and nickel layers were in the low-10^{-8} torr range. Both the copper and nickel growth rates

 ©1999 The American Physical Society

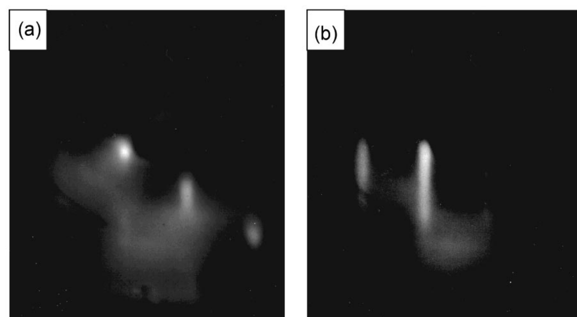

FIG. 1. RHEED patterns recorded from a Cu(2000 Å)/Si(001) surface in the [200] azimuth: (a) is the surface of the copper without the intentional anneal; (b) is the surface after the copper was annealed at 200 °C for about one minute.

were 1.0 Å/s. Film growth started at a temperature of 20 °C and substrate temperature gradually increased to about 50 °C during the deposition due to the thermal radiation from the sources. Reflected high-energy electron diffraction (RHEED) was used to monitor the film quality *in situ*. The copper buffer layers for all the samples except the 500 and 2000 Å films were annealed *in situ* to about 150 °C for eight minutes and then cooled down to 20 °C prior to the deposition of the nickel layer. The annealing process improved the flatness of the buffer layer surface. Figure 1(a) shows the RHEED pattern of a 2000 Å copper film on Si(001) before the anneal. The spottedness of the pattern indicates that the surface of the copper film was atomically rough. Figure 1(b) shows the RHEED pattern of the same film after the anneal. The streaky RHEED pattern suggests that the the surface was atomically flat. The surface retains its smoothness after the deposition of the nickel and copper capping layer as confirmed by RHEED patterns.

Annealing of epitaxial Cu(2000 Å)/Si(001) films above 200 °C appears to cause the formation of copper silicide through the copper buffer layer. Figure 2 is a scanning electron micrograph of a Cu(2000 Å)/Si(001) film that was annealed at around 200 °C for about a minute. The image shows islands of copper silicide on the copper film as indicated by Auger spectroscopy and microanalysis. X-ray study confirms that at least some of the silicide was $Cu_{15}Si_4$, as discussed later in the paper. However, no silicon could be detected by Auger spectroscopy on the surface of the copper

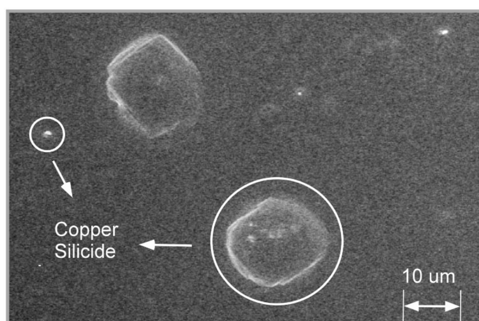

FIG. 2. Scanning electron microscopy image of Cu(2000 Å)/Si(001) film annealed at 200 °C for about one minute. Islands of copper silicide threaded through the copper layer. The islands come in two sizes.

buffer layer that was annealed *in situ* at 150 °C for less than eight minutes.

III. EXPERIMENTAL RESULTS AND ANALYSES

The x-ray experiments were performed using the beamline X3B1 of the Brookhaven National Synchrotron Light Source. Synchrotron radiation was used for its high intensity and narrow collimation. The wavelength of the radiation was selected to be 1.149 Å by a double-crystal Si(111) monochromator; the scattered x-rays were analyzed by a Ge(111) crystal to provide high-angular resolution. Both the Bragg and grazing-incidence diffraction setups were calibrated using an Al_2O_3 powder reference standard. The resolutions for both setups were on the order of 0.02° in scattering angle 2θ.

Diffraction from the copper buffer layer was used to align the sample with the incident beam for both the in-plane and out-of-plane lattice measurements. Since the lattice orientation of the copper buffer layer is known with respect to the silicon substrate, namely Si⟨110⟩‖Cu⟨100⟩,[11,12] the detector was first set at an expected scattering angle 2θ. The sample was rocked about the angle 2θ with respect to the incident beam to maximize the intensity at the detector. The condition of maximum intensity is a Bragg condition. The crystal was then aligned by setting $\theta=\theta_{\max}$. Once the copper film is aligned, the nickel is also aligned by virtue of its epitaxial growth on the copper, Cu⟨100⟩‖Ni⟨100⟩. This epitaxial relationship between the nickel and copper is confirmed by the diffraction experiments, as discussed below.

A. Symmetric Bragg diffraction

The out-of-plane lattice constant of the nickel, $a_{\perp}^{\mathrm{Ni}}$, was measured using the symmetric Bragg diffraction method. The intensities from the (002) planes of the copper and nickel are shown in Fig. 3. Note the logarithmic scale in the *y* axis. The copper peak position stays at its bulk value for all the nickel film thicknesses; the nickel peak evolves toward its bulk value with the increasing nickel film thickness. The 500 and 2000 Å films still show significant vertical contraction, signifying that they are not fully relaxed.

There is a peak between that of the copper and nickel, which is particularly pronounced for the thinner films. We believe it comes from the diffraction by the (521) planes of the ϵ-$Cu_{15}Si_4$ cubic phase, which is buried in the Cu buffer layer, near the Cu/Si interface. The *d* spacing calculated from the diffraction peak is 1.756 Å; the reported value in the literature is 1.767 Å.[13] Other peaks of the $Cu_{15}Si_4$ phase were also detected in the annealed samples using a laboratory source with Cu K_α radiation. However, it must be pointed out that other workers had reported the copper silicide at the Cu/Si interface to be η''-Cu_3Si phase.[11,12,14]

For the thinner nickel films ($30\,\mathrm{Å}\leqslant t_{\mathrm{Ni}}\leqslant 150\,\mathrm{Å}$), since there is a large difference in the intensity between the copper and nickel peak, the fitting of the nickel peak is very sensitive to the profile of the tail of the copper peak. The following procedure was used to extract the nickel diffraction data: the copper peak was first fitted with more weight being placed on its left tail. The fitting was best achieved with a mixture of a gaussian and lorentzian function. The fitted curve was then used to subtract the copper contribution from

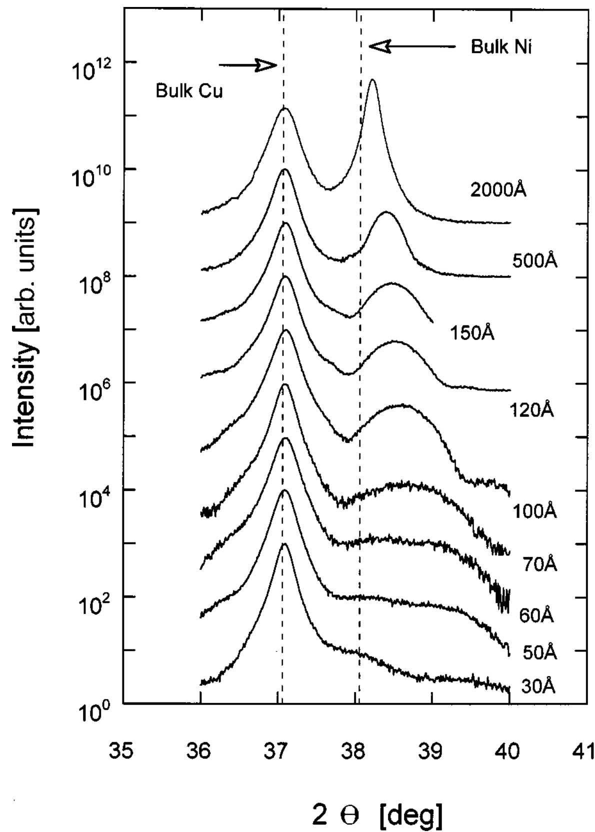

FIG. 3. X-ray reflectivity from the (002) Bragg planes of the copper and nickel layer in Cu/Ni/Cu/Si(001) films. The wavelength of the radiation is 1.149 Å. All curves are displaced by arbitrary amounts.

the reflectivity data. The remaining intensity was assumed to be that of the nickel and $Cu_{15}Si_4$, each of which was fitted with a gaussian. For the 500 or 2000 Å nickel film, both the nickel and copper capping layer were fitted simultaneously with strictly Gaussian functions. The intensity from the copper silicide can be safely neglected for these two nickel film thicknesses. The computed lattice constants (using the Bragg formula) are tabulated in Table I. It must be said that the contribution of the copper capping layer was ignored in the analysis. The capping layer peak is so weak that the buffer-copper peak overlaps it completely and therefore hinders the determination of the lattice constant of the capping copper layer.

As expected from epitaxial (002) films, no (111) diffraction peaks could be detected in the $\theta-2\theta$ scan. Further, the grazing-incidence diffraction confirms true epitaxy between the Ni and Cu layers, as we shall now discussed.

B. Grazing-incidence diffraction

The in-plane lattice constant of the nickel was measured in the grazing-incidence diffraction (GID) geometry.[15] In this setup, the sample plane is inclined slightly from the vertical scattering plane (defined by the incident beam and the center of the detector). The incident beam meets the surface at a grazing angle γ of 0.3 to 0.6°, while the detector accepts radiation from the grazing exit angle between zero and about one degree. The diffraction from Bragg planes that are exactly or nearly perpendicular to the surface of the sample is collected. Figure 4 shows the intensity diffracted from the (200) planes with $\gamma=0.6°$. As before, the peak of the the copper buffer layer (if observed) stays at its bulk value for all the nickel films, and the nickel peak evolves toward its bulk value with the increasing nickel film thickness. Note that the (521) $Cu_{15}Si_4$ peak was not observed in grazing incidence,

TABLE I. In- and out-of-plane nickel lattice constants ($a_{\parallel}$ and $a_{\perp}$ with estimated errors of ±0.005 Å) are tabulated for the various nickel film thicknesses using the (200) and (002) diffraction peaks, respectively. Strains (±10%) are computed by using the formula $(a-a_b)/a_b$ where a_b (=3.5241 Å) is the bulk lattice constant of nickel. The in-plane strains are calculated using the $\gamma=0.6°$ data except for the 50 and 70 Å films, the $\gamma=0.3°$ data are used to calculate the strains. The value for $2c_{12}/c_{12}$ is found by taking the ratio of $\epsilon_{\perp}$ to $\epsilon_{\parallel}$.

t_{Ni} [Å]	$a_{\perp}$ [Å]	$\epsilon_{\perp}$ [%]	$a_{\parallel}$ [Å] ($\gamma=0.6°$)	$a_{\parallel}$ [Å] ($\gamma=0.3°$)	$\epsilon_{\parallel}$ [%]	$-2c_{12}/c_{11}$
30	3.4180	−3.01	3.6038		2.26	1.33
50	3.4433	−2.30	3.5884	3.5908	1.89	1.21
60	3.4514	−2.07	3.5878		1.81	1.14
70	3.4604	−1.82	3.5774	3.5767	1.49	1.21
100	3.4779	−1.31	3.5652		1.17	1.12
120	3.4834	−1.15	3.5626		1.09	1.06
150	3.4873	−1.04	3.5557		0.90	1.16
500	3.4945	−0.84	3.5482		0.68	1.23
2000	3.5107	−0.38	3.5353		0.32	1.20

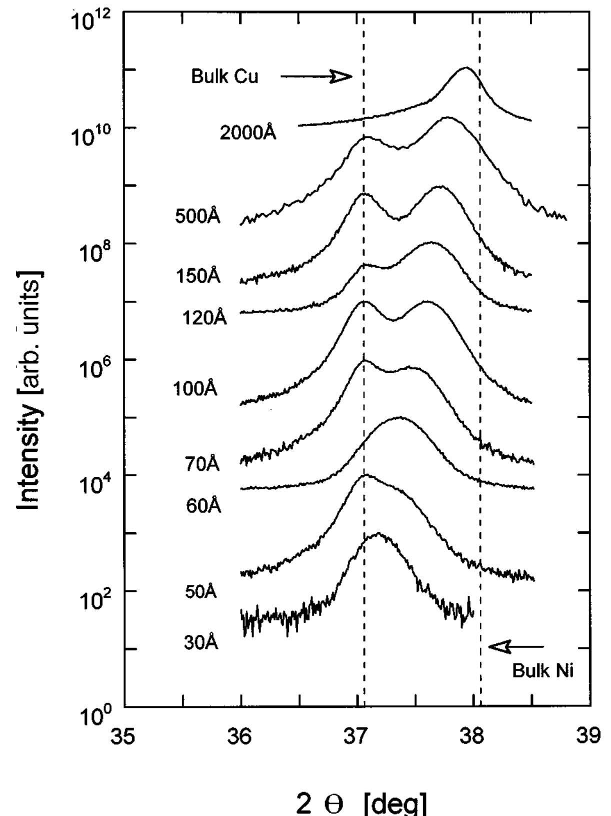

FIG. 4. Grazing incidence diffraction (with $\gamma=0.6°$) from the (200) Bragg planes of the copper and nickel layer in Cu/Ni/Cu/Si(001) films. The wavelength of the radiation is 1.149 Å. All curves are displaced by arbitrary amounts.

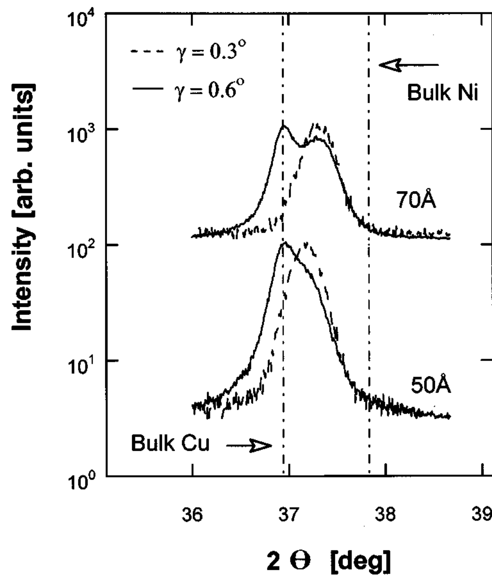

FIG. 5. Grazing incidence diffraction from the (200) Bragg planes of the copper and nickel layer in Cu/Ni/Cu/Si(001) films at two incident angles (0.3° and 0.6°). The wavelength of the radiation is 1.149 Å. All curves are displaced by arbitrary amounts.

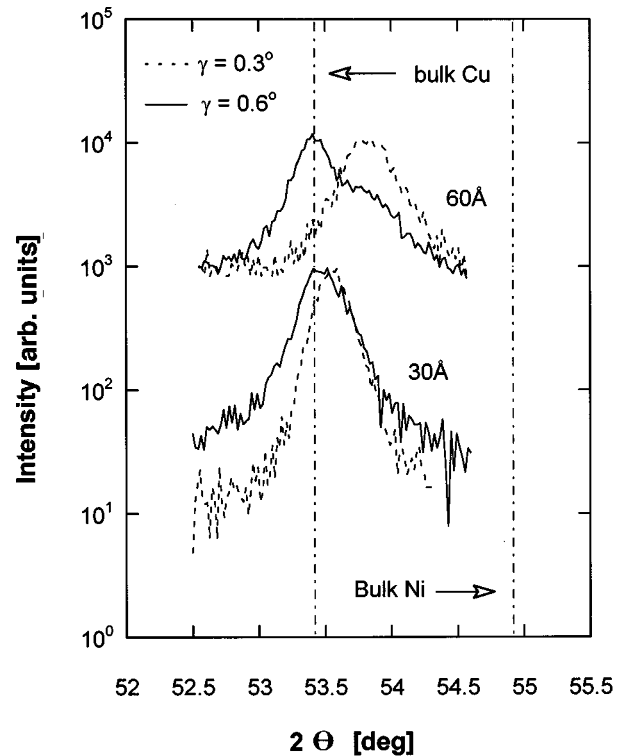

FIG. 6. Grazing incidence diffraction from the (220) Bragg planes of the copper and nickel layer in Cu/Ni/Cu/Si(001) films at two incident angles (0.3° and 0.6°). The wavelength of the radiation is 1.149 Å. All curves are displaced by arbitrary amounts.

which suggests that the silicide is buried well below the nickel/copper buffer interface.

The penetration depth of the radiation could be varied by changing the grazing angle γ.[16] Figure 5 shows the diffracted intensity of the 50 and 70 Å nickel films with two different values of γ (0.3° and 0.6°). Very little scattered intensity was observed from the copper buffer layer for $\gamma=0.3°$. These results show, as expected, that the diffraction intensity is very sensitive to the γ parameter. It must be said that there is a considerable error ($\pm 0.1°$) in determining the absolute value of γ. The major source of the error comes from the mounting of the sample that might not be completely flat on the sample holder.

The GID intensities were fitted with Gaussian functions. Since the diffracted intensity from the copper layer is comparable to that of the thin-nickel film due to the shallowness of the incident angle γ, both peaks were analyzed at the same time. For the cases with $\gamma=0.3°$, only one gaussian was needed. We assume the capping layer is completely coherent with the nickel for nickel thicknesses below 150 Å. Thus, the contribution of the copper capping layer was ignored in the fitting, except for the 2000-Å Ni film data, where there is a clear peak asymmetry that we attributed to the capping layer. The computed in-plane lattice constants are tabulated in Table I.

The diffraction from the (220) Bragg planes was also studied by GID on the 30- and 60-Å nickel films. Figure 6 shows the diffraction intensity of these samples with $\gamma=0.3°$ and 0.6°. The in-plane lattice constants calculated from these (220) peaks are in good agreement which those was found from the (200) peaks, and they are tabulated in Table II. One advantage of using the (220) peaks is that they show more separation than do the (200) peaks. For bulk copper and nickel, the separation is 1.5° for the (220) peaks and 1.0° for the (200) peaks. The disadvantage is that the intensity of the former is about half of that of the latter.

To confirm that these films are indeed epitaxial (002) films (as opposed to just highly textured films), the incident x-ray beam was deliberately misaligned (about a few degrees) away from a [100] crystallographic direction of Ni. Then, the (200) and (220) peaks were scanned. As expected, no diffraction peaks could be detected.

IV. DISCUSSION

Epitaxial nickel on copper is under a biaxial tensile stress due to the lattice mismatch in their bulk forms. The lattice mismatch gives rise to isotropic strain in the (001) plane ($\epsilon_{xx}=\epsilon_{yy}\equiv\epsilon_{\parallel}$), and an out-of-plane compressive strain [$\epsilon_{\perp}=-(2c_{12}/c_{11})\epsilon_{\parallel}$] due to the Poisson effect. The misfit strain of nickel on copper is 2.6%. Figure 7 shows both the in-plane and out-of-plane average residual strain of the nickel layer as a function of the nickel film thickness. The strains are calculated using the formula $(a-a_b)/a_b$ where a is the

TABLE II. In-plane lattice constants ($a_{\parallel}$ with estimated errors of ± 0.005 Å) were calculated using the (220) diffraction peaks with $\gamma=0.3°$ and 0.6°. The strain ($\pm 10\%$) is calculated using the formula $(a-a_b)/a_b$ where a_b ($=3.5241$ Å) is the bulk lattice constant of nickel.

t_{Ni} [Å]	γ	$a_{\parallel}$	$\epsilon_{\parallel}$ [%]
30	0.3	3.6066	2.34
30	0.6	3.6016	2.20
60	0.3	3.5894	1.85
60	0.6	3.5912	1.90

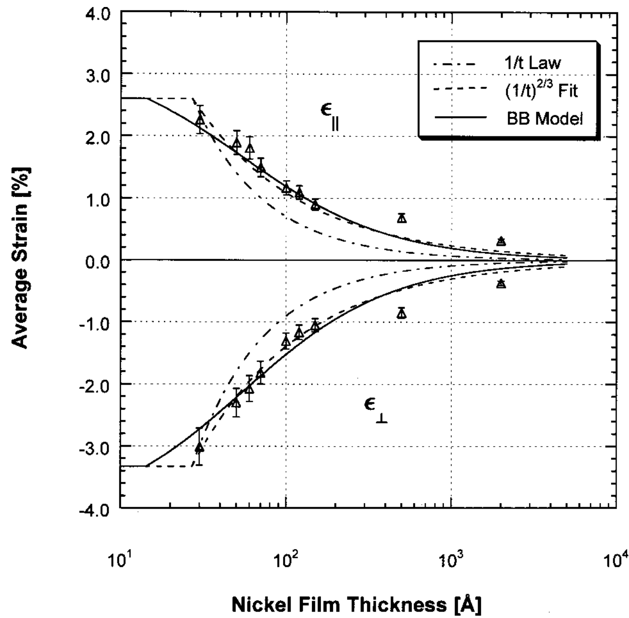

FIG. 7. In-plane and out-of-plane strain as a function of the nickel film thickness. The data are fitted with three different models: the $1/t$ law, $(1/t)^{2/3}$ fit, and Basson and Ball equilibrium model.

measured lattice constant, and $a_b = 3.5241$ Å, is the bulk lattice constant of nickel.[17] The values are also given in Table I. The ratio $-\epsilon_\perp/\epsilon_\parallel$ has the value 1.18 ± 0.05, which is very close to the ratio in a bulk nickel crystal, $2c_{12}/c_{11} = 1.28$ (Ref. 18) (see Table I). The relarionship between $-\epsilon_\perp/\epsilon_\parallel$ and $2c_{12}/c_{11}$ can be found using the strain-stress relationships, using the fact that the stress along the axial direction, $\sigma_{zz} = 0$ in the nickel film. The Poisson's ratio ν is calculated to be 0.37 ± 0.1 using the formula $2c_{12}/c_{11} = 2\nu/(1-\nu)$.

One simple way of analyzing and predicting the thickness dependence of the strain is to first fit the in-plane strain data (better resolution than out-of-plane) using the phenomenological equation $\epsilon_\parallel = \eta(t_c/t_{\rm Ni})^p$ where $\eta(=2.6\%)$ is the misfit strain of the nickel on copper, t_c and p are the fitting parameters. With $t_c = 27$ Å, and $p = 2/3$, the power law gives a good fit to the data (see Fig. 7), if it is restricted only to films that are less than 150-Å thick. The out-of-plane strain curve found by the formula $\epsilon_\perp = -(2c_{12}/c_{11})\eta(t_c/t_{\rm Ni})^p$, is in good agreement with the experimental result. A natural interpretation, coming from the dimensionality of the parameter t_c is that it is the critical thickness below which the nickel is coherent with the copper buffer layer. But it must be warned that there is no theoretical basis to think that this is indeed the true critical thickness (in fact, it is not, as we shall see). One justification for restricting the nickel thicknesses range in the fitting is that both the in plane and out of plane strain are better fitted if the data from the 500 and 2000 Å film are excluded. A better justification comes from an equilibrium theory, which is now discussed.

Thermodynamic equilibrium theory of misfit strain relaxation in epitaxial films is based on minimizing elastic and dislocation energy. The method was first introduced by Frank and van der Merwe in 1949.[19] The model proposed by Basson and Ball (the BB model) (Ref. 9) is an extension of the Matthews model[10] from single to multilayered films. Since the capping layered film thickness is comparable to that of the nickel film, it seems appropriate to employ the BB model in analyzing the strain data. With some assumptions (which will be stated later), the equilibrium value of in-plane biaxial strain, as predicted by the BB model, can be obtained using the following equation:

$$\epsilon_\parallel^3 = \frac{b}{\cos\psi\sin\beta}\,\frac{(1-\nu\cos^2\beta)}{8\pi(1+\nu)}\,\frac{1}{t_{\rm Cu}+t_{\rm Ni}}\ln\left(\frac{t_{\rm Cu}+t_{\rm Ni}}{b/\alpha}\right) + \frac{t_{\rm Cu}}{t_{\rm Cu}+t_{\rm Ni}}\eta \qquad (1)$$

Here, b is the length of the Burgers vector, $t_{\rm Cu}$ is the cap copper film thickness. ψ is the angle between the interfacial plane and the slip plane of the dislocation; β the angle between the Burgers vector and dislocation lines. α is an *ad hoc* factor to account for the core energy of a dislocation. For metals, its value is between 0.5 and 2;[20] $\alpha = 1$ is used in our analysis. The first term in Eq. (1) can be interpreted as the strain of the film whose thickness is the sum of the film thicknesses of the copper capping and nickel layer; the second term accounts for the fact that copper and nickel have different bulk lattice constants, weighed by the thickness of the capping layer. Notice that for $t_{\rm Cu} = 0$, we get the Matthews' expression for the strain of a single epilayer,[10] as expected.

The assumptions used in writing Eq. (1) are: (i) the films are mechanically isotropic; (ii) both the nickel and copper capping layer have the same Poisson's ratio and shear modulus; (iii) the copper capping layer is completely coherent with the nickel. Although the BB model makes a distinction between cases for which the average linear spacing of the dislocation s is greater or less than twice the total film thickness $2(t_{\rm Cu}+t_{\rm Ni})$, we find that the difference is not significant for our films. For simplicity, we assume the case $s > 2(t_{\rm Cu} + t_{\rm Ni})$ for all nickel-film thicknesses.

If the dislocations in the nickel are assumed to be purely 60° dislocations on {111} slip planes, then $\cos\psi = 1/\sqrt{3}$, $\cos\beta = 1/2$, and $b = a_{\rm Ni}/\sqrt{2}$, where $a_{\rm Ni}$ is the lattice constant of the nickel layer. Using these numbers, the in-plane equilibrium strain can be found, and it is plotted in Fig. 7 (BB model). The equilibrium critical thickness of the nickel t_c^e (the thickness below which it is energetically more favorable for the nickel film to be coherent on the copper buffer layer) is calculated to be 15 Å using Eq. (1) with $\epsilon_\parallel^e = 2.6\%$. This is in agreement with the result reported by Inglefield,[21] which is that t_c must be between 15 to 20 angstroms. The out-of-plane strain is found by the formula $\epsilon_\perp = -(2c_{12}/c_{11})\epsilon_\parallel$. Note that for the thinner nickel films, the predicted equilibrium strains agree well with the measured values. This is expected because the misfit strain between the nickel and copper is large (2.6%). However, the thicker films (500 and 2000 Å) show large deviation from the equilibrium strain, which is in agreement with other studies.[6,7] The reason for this departure is not well understood. It has been argued by Matthews and Crawford[6] that the misfit dislocations have not reached their equilibrium density due perhaps to the tangling of dislocations. Figure 7 also shows the $1/t$ curve using $t_c = 27$ Å. The critical thickness of 27 Å (instead of 15 Å) is used for two reasons: (i) a useful comparison with the $(1/t)^{2/3}$ law can be made; (ii) it gives better fit than that if

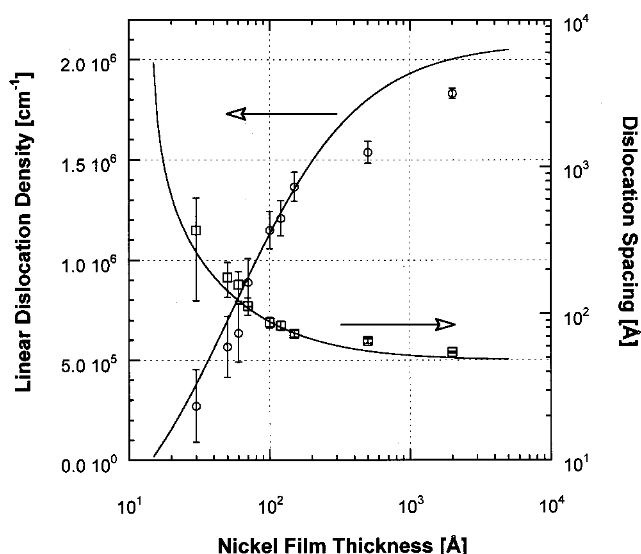

FIG. 8. The solid line is the equilibrium linear density of dislocation. The dash line is the equilibrium dislocation spacing. These lines come from the Basson and Ball model. The discrete points are the data calculated from the diffraction peaks.

$t_c = 15$ Å is used. Observe that the strain predicted by the $1/t$ law drops much faster than that of the experimental values and the BB model. The failure of the $1/t$ law, as it is applied in this system, is due mainly to the exclusion of the influence of the capping layer in its derivation.

The linear dislocation density ρ can be estimated from the strain data using the following formula[22]

$$\rho = \frac{\eta - \epsilon_{\parallel}}{b \sin \beta \cos \psi} \tag{2}$$

The result for both the equilibrium and measured dislocation densities are plotted in Fig. 8. As expected, the dislocations densities increase with increasing nickel film thickness to reduce the strain energy. The dislocation spacing, $s = 1/\rho$, is also plotted on the same figure.

V. CONCLUSIONS

The strain in a series of Cu/Ni/Cu/Si(001) films has been studied using x-ray diffraction. Perpendicular and in-plane strains of the nickel films have been measured independently using symmetric Bragg and grazing-incidence diffraction respectively. The 2000 Å copper buffer layer maintains its bulk lattice constnat, even with nickel films that are up to 2000 Å in thickness. The Ni misfit strain decrease approximately as $(1/t)^{2/3}$ rather than the often assumed $1/t$ form. Its absolute values are significantly larger than those previously reported. The BB equilibrium model seems to be able to account for the strain in the nickel films that are less than 150 Å thick. The equilibrium critical thickness is predicted to be about 15 Å. The ratio of out-of-plane and in-plane strain agrees well with the bulk value. The strain in thicker Ni films (500 and 2000 Å) is appreciably larger than equilibrium strain, in agreement with the earlier work.

ACKNOWLEDGMENTS

The films were grown at MIT as part of National Science Foundation (NSF) Grant No. DMR 9410943. M.C. is grateful to the Spanish Ministerio de Educacion for financial support. The diffraction experiments were carried out at the National Synchrotron Light Source at Brookhaven National Laboratory, which is supported by the U.S. Department of Energy, Division of Materials Sciences and Division of Chemical Sciences under Grant No. DE-FG02-86ER45231.

[1] R. Jungblut, M. T. Johnson, J. aan de Stegge, A. Reinders, and F. J. A. den Broeder, J. Appl. Phys. **75**, 6424 (1994).
[2] Gabriel Bochi, C. A. Ballentine, H. E. Inglefield, C. V. Thompson, and R. C. O'Handley, Phys. Rev. B **53**, 1729 (1996).
[3] K. Ha and R. C. O'Handley, J. Appl. Phys. **85**, 5282 (1999).
[4] C.-A. Chang, J. Appl. Phys. **68**, 4873 (1990).
[5] S. Müller, B. Schulz, G. Kostka, M. Farle, K. Heinz, and K. Baberschke, Surf. Sci. **364**, 235 (1996).
[6] J. W. Matthews and J. L. Crawford, Thin Solid Films **5**, 187 (1970).
[7] U. Gradmann, Ann. Phys. (N.Y.) **7**, 161 (1966).
[8] C. Chappert and P. Bruno, J. Appl. Phys. **64**, 5736 (1988).
[9] J. H. Basson and C. A. B. Ball, Phys. Status Solidi A **46**, 707 (1978).
[10] W. A. Jesser and J. W. Matthews, Philos. Mag. **15**, 1097 (1967).
[11] B. G. Demczyk, R. Naik, G. Auner, C. Kota, and U. Rao, J. Appl. Phys. **75**, 1956 (1994).
[12] C.-A. Chang, Appl. Phys. Lett. **57**, 2239 (1990).
[13] K. P. Mukherjee, J. Bandyopadhyaya, and K. P. Gupta, Trans. Am. Inst. Min., Metall. Pet. Eng. **245**, 2335 (1969).
[14] G. Weber, G. Billot, and P. Barret, Phys. Status Solidi A **75**, 567 (1983).
[15] W. C. Marra, P. Eisenberger, and A. Y. Cho, J. Appl. Phys. **50**, 6927 (1979).
[16] I. C. Noyan, T. C. Huang, and B. R. York, Crit. Rev. Solid State Mater. Sci. **20**, 125 (1995).
[17] A. Taylor and B. J. Togle, *Crystallographic Data on Metal and Alloy Structures*, (Dover, New York, 1962).
[18] J. F. Nye, *Physical Properties of Crystals* (Oxford University Press, Oxford, 1967).
[19] F. C. Frank and J. H. van der Merwe, Proc. R. Soc. London, Ser. A **198**, 205 (1949); **198**, 216 (1949).
[20] J. P. Hirth and J. Lothe, *Theory of Dislocations* (McGraw-Hill, New York, 1968), p. 212.
[21] H. E. Inglefield, Ph.D. thesis, Massachusetts Institute of Technology, 1995.
[22] J. Y. Tsao, *Materials Fundamentals of Molecular Beam Epitaxy* (Academic, New York, 1993), p. 164.